REPORT DOCUMENTATION PAGE

Form Approved
OMB No. 0704-0188

1. REPORT DATE *(DD-MM-YYYY)*	2. REPORT TYPE	3. DATES COVERED *(From - To)*
01-05-2004	Journal Article	2003

4. TITLE AND SUBTITLE
Statistical analysis of the non-homogeneity detector for STAP applications

5a. CONTRACT NUMBER
N/A

5b. GRANT NUMBER
N/A

5c. PROGRAM ELEMENT NUMBER
61102F

6. AUTHOR(S)
Muralidhar Rangaswamy, Air Force Research Laboratory/SNHE, James H. Michels, and Braham Himed, Air Force Research Laboratory/SNRT

5d. PROJECT NUMBER
2304

5e. TASK NUMBER
HE

5f. WORK UNIT NUMBER
2304HE01

7. PERFORMING ORGANIZATION NAME(S) AND ADDRESS(ES)
Electromagnetic Scattering Branch (AFRL/SNHE)
80 Scott Drive,
Hanscom AFB, MA 01731-2909

8. PERFORMING ORGANIZATION REPORT NUMBER
N/A

9. SPONSORING/MONITORING AGENCY NAME(S) AND ADDRESS(ES)
Sensors Directorate
Source Code: 437890
Electromagnetic Technology Division
80 Scott Drive
Hanscom AFB, MA 01731-2909

10. SPONSOR/MONITOR'S ACRONYM(S)
AFRL-SN-HS

11. SPONSOR/MONITOR'S REPORT NUMBER(S)
AFRL-SN-HS-JA-2001-1438

12. DISTRIBUTION/AVAILABILITY STATEMENT
APPROVED FOR PUBLIC RELEASE, DISTRIBUTION UNLIMITED.

13. SUPPLEMENTARY NOTES
Supported by Air Force Office of Scientific Research (AFOSR); ESC Public Affairs Clearance #: 01-1438

14. ABSTRACT
We present a statistical analysis of the recently proposed non-homogeneity detector (NHD) for Gaussian interference statistics. Specifically, we show that a formal goodness-of-fit test can be constructed by accounting for the statistics of the generalized inner product (GIP) used as the NHD test statistic. The normalized-GIP follows a central-F distribution and admits a canonical representation in terms of two statistically independent chi-squared distributed random variables. Moments of the GIP can be readily calculated as a result. These facts are used to derive the goodness-of-fit tests, which facilitate intelligent training data selection. We then address the issue of space–time adaptive processing (STAP) algorithm performance using the NHD as a pre-processing step for training data selection. Performance of the adaptive matched filter (AMF) method is reported using simulated as well as measured data.

15. SUBJECT TERMS
STAP, Non-homogeneous detector, F-distribution, Goodness-of-fit test, GIP, AMF, False alarm probability, Detection probability, Signal-to-noise-ratio (SNR)

16. SECURITY CLASSIFICATION OF:			17. LIMITATION OF ABSTRACT	18. NUMBER OF PAGES	19a. NAME OF RESPONSIBLE PERSON
a. REPORT	b. ABSTRACT	c. THIS PAGE			Muralidhar Rangaswamy
U	U	U	UU	16	19b. TELEPHONE NUMBER *(Include area code)*

Available online at www.sciencedirect.com
SCIENCE DIRECT®
Digital Signal Processing 14 (2004) 253–267
Digital Signal Processing
www.elsevier.com/locate/dsp

Statistical analysis of the non-homogeneity detector for STAP applications

Muralidhar Rangaswamy,[a,*] James H. Michels,[b] and Braham Himed[b]

[a] *Air Force Research Laboratory/SNHE, 80 Scott Drive, Hanscom Air Force Base, MA 01731-2909, USA*
[b] *Air Force Research Laboratory/SNRT, 26 Electronic Parkway, Rome, NY 13441-4514, USA*

Abstract

We present a statistical analysis of the recently proposed non-homogeneity detector (NHD) for Gaussian interference statistics. Specifically, we show that a formal goodness-of-fit test can be constructed by accounting for the statistics of the generalized inner product (GIP) used as the NHD test statistic. The normalized-GIP follows a central-F distribution and admits a canonical representation in terms of two statistically independent chi-squared distributed random variables. Moments of the GIP can be readily calculated as a result. These facts are used to derive the goodness-of-fit tests, which facilitate intelligent training data selection. We then address the issue of space–time adaptive processing (STAP) algorithm performance using the NHD as a pre-processing step for training data selection. Performance of the adaptive matched filter (AMF) method is reported using simulated as well as measured data.

Keywords: STAP; Non-homogeneity detector; F-distribution; Goodness-of-fit test; GIP; AMF; False alarm probability; Detection probability; Signal-to-noise-ratio (SNR)

1. Introduction

An important issue in space–time adaptive processing (STAP) for radar target detection is the formation and inversion of the covariance matrix underlying the clutter and interference. Typically, the unknown interference covariance matrix is estimated from a set of independent identically distributed (iid) target-free training data that is representative of the interference statistics in a cell under test. Frequently, the training data is subject to

* Corresponding author.
E-mail addresses: muralidhar.rangaswamy@hanscom.af.mil (M. Rangaswamy), james.michels@rl.af.mil (J.H. Michels).

1051-2004/$ – see front matter
doi:10.1016/S1051-2004(03)00021-6

contamination by discrete scatterers or interfering targets. In either event, the training data becomes non-homogeneous. Consequently, it is not representative of the interference in the test cell. Estimates of the covariance matrix from non-homogeneous training data result in severely under-nulled clutter. Consequently, CFAR and detection performance suffer. However, significant performance improvement can be achieved by employing a pre-processing technique to select representative training data.

The problem of target detection using improved training strategies has been considered in [6,7,14,15]. The impact of non-homogeneity on STAP performance is considered in [10,16,17,19]. It was shown in [21] that the distribution information of a class of multivariate probability density functions (PDF) is succinctly determined through an equivalent univariate PDF of a quadratic form. An application of this result is the non-homogeneity detector (NHD) based on the generalized inner product (GIP) [6,7,10,14,15].

Non-homogeneity of the training data arises due to a number of factors such as contaminating targets, presence of strong discretes, and non-stationary reflectivity properties of the scattering surface. In these scenarios, the test cell disturbance covariance matrix, $\mathbf{R}_T$, differs significantly from the estimated covariance matrix, $\widehat{\mathbf{R}}$, formed using target-free disturbance realizations from adjacent reference cells. If a large number of test cell data realizations are available, the underlying non-homogeneity is characterized via the eigenvalues of $\widehat{\mathbf{R}}^{-1}\mathbf{R}_T$ [8]. However, in radar applications, only a single realization of test cell data is usually available. Consequently, the resulting estimate of $\mathbf{R}_T$ is singular. Hence, [6,7,10,14,15] compared the empirically formed GIP with a theoretical mean corresponding to a "known" covariance matrix. Large deviations of the GIP mean value from the theoretical mean have been ascribed to non-homogeneity of the training data. Such an approach provides meaningful results in the limit of large training data size. In practice, the amount of training data available for a given application is limited by system considerations such as bandwidth and fast scanning arrays. Furthermore, the inherent temporal and spatial non-stationarity of the interference precludes the collection of large amounts of training data. Consequently, the approach of [6,7,10,14,15] can be misleading since it ignores finite data effects and the resulting variability in the covariance matrix estimate [20]. Specifically, we note that the empirical GIP mean using an estimated covariance matrix with finite data can be twice as large as the corresponding GIP mean for a known covariance matrix in some instances. Consequently, such a scenario can easily lead to incorrect classification of training data.

The normalized GIP, P', admits a remarkably simple stochastic representation as the ratio of two statistically independent chi-square distributed random variables [20]. Consequently, the normalized GIP follows a central-F distribution [1,4,24]. The main result of this paper lies in exploiting these facts to construct a formal goodness-of-fit test for selecting homogeneous training data and its application to the performance of the adaptive matched filter (AMF) test [5,9,22]. Other applications of the F-distribution can be found in [2,3,12].

Section 2 briefly reviews the GIP statistics for the case of a known covariance matrix. In Section 3 we discuss the GIP statistics for the case of an unknown covariance matrix. Section 4 introduces the non-homogeneity detector and derives formal goodness-of-fit tests based on the GIP statistics described in Section 3. The AMF test performance with and without training data contamination using simulated and measured data is presented in

Section 5. The AMF performance is shown to degrade with contaminated training data. It is further shown in Section 5 that the use of NHD pre-processing enables selection of representative training data. Consequently, use of NHD pre-processing restores the AMF test performance to case where there is no training data contamination.

2. GIP statistics: known covariance matrix

Let $\mathbf{x} = [x_1, x_2, \ldots, x_M]^T$ denote a complex random vector with zero mean and known positive definite Hermitian covariance matrix $\mathbf{R}$. The quadratic form given by

$$Q = \mathbf{x}^H \mathbf{R}^{-1} \mathbf{x} \tag{2.1}$$

has the important property [20]

$$E(Q) = M. \tag{2.2}$$

This result is important in that it is independent of the PDF underlying $\mathbf{x}$ and is only a function of the dimension of the random vector. If the PDF of $\mathbf{x}$ is known, the corresponding PDF of Q can be readily derived. For Gaussian distributed $\mathbf{x}$, i.e., $\mathbf{x} \sim CN(0, \mathbf{R})$, the PDF of Q is a chi-squared distribution with M complex degrees of freedom. More precisely the PDF of Q is given by

$$f_Q(q) = \begin{cases} \dfrac{q^{M-1}}{\Gamma(M)} \exp(-q) & q \geqslant 0 \\ 0 & \text{otherwise} \end{cases} \tag{2.3}$$

where $\Gamma(.)$ is the Euler-Gamma function.

The GIP based NHD calculates the quadratic form Q using an estimated covariance matrix (formed from iid target free training data) and compares its mean with M. Deviations from M have been attributed to non-homogeneities in the training data [6,7,10,14,15]. In practice, the interference covariance matrix is formed from a finite amount of training data. The statistical variability associated with the data could introduce additional errors and thus, deviations of the GIP from M cannot entirely be ascribed to the presence of non-homogeneities. Consequently, it is useful to work with the statistics of Q formed with an estimated covariance matrix with finite sample support. The GIP PDF and moments are quite different from those of Eqs. (2.2) and (2.3) for the finite sample support problem.

3. GIP statistics: unknown covariance matrix

Let $\mathbf{x} \sim CN(0, \mathbf{R}_T)$ denote the test data vector and $\mathbf{Z}$ denote a data matrix, whose columns $\mathbf{z}_k$, $k = 1, 2, \ldots, K$, are iid $CN(\mathbf{0}, \mathbf{R})$ target-free training data vectors. For homogeneous (representative) training data, $\mathbf{R}_T = \mathbf{R}$. The sample covariance matrix given by $\widehat{\mathbf{R}} = \frac{1}{K}\mathbf{Z}\mathbf{Z}^H$ is the maximum likelihood estimate of the covariance matrix. Let

$$P = \mathbf{x}^H \widehat{\mathbf{R}}^{-1} \mathbf{x}. \tag{3.1}$$

We derive a canonical stochastic representation for the normalized GIP, $P' = P/K$, in terms of two statistically independent chi-squared distributed random variables in Appendix A. Consequently, we have

$$P = \frac{R_1}{R_2/K}, \tag{3.2}$$

where R_1 and R_2 are statistically independent chi-squared distributed random variables with PDFs given by

$$f_{R_1}(r_1) = \begin{cases} \dfrac{r_1^{M-1}}{\Gamma(M)} \exp(-r_1) & r_1 \geqslant 0 \\ 0 & \text{otherwise} \end{cases} \tag{3.3}$$

$$f_{R_2}(r_2) = \begin{cases} \dfrac{r_2^{K-M}}{\Gamma(K-M+1)} \exp(-r_2) & r_2 \geqslant 0 \\ 0 & \text{otherwise} \end{cases} \tag{3.4}$$

respectively. Consequently, P' follows a central-F distribution [1,4,24] given by

$$f_{P'}(p') = \begin{cases} \dfrac{(p')^{M-1}}{\beta(M,L)(1+p')^{L+M}} & p' \geqslant 0 \\ 0 & \text{otherwise} \end{cases} \tag{3.5}$$

where $\beta(M,L) = \int_0^1 \varsigma^{M-1}(1-\varsigma)^{L-1}\, d\varsigma$ and $L = K - M + 1$.

The statistical equivalence of P' to the ratio of two independent chi-squared distributed random variables is fascinating in that it permits rapid calculation of the moments of P. More importantly, it is extremely useful in Monte-Carlo studies involving computer generation of P. For homogeneous training data, the use of (3.2) circumvents the need to explicitly generate the test data vector $\mathbf{x}$ and the training data vectors used for covariance estimation. For large M and perforce K, significant computational savings can be realized from the method of (3.2). It can be readily shown that

$$E(P) = \frac{M}{\left(1 - \frac{M}{K}\right)}, \tag{3.6}$$

$$\mathrm{Var}(P) = \sigma_P^2 = \frac{M}{\left(1 - \frac{M}{K}\right)^2\left[1 - \frac{(M+1)}{K}\right]}, \tag{3.7}$$

where $E(P)$ and $\mathrm{Var}(P)$ denote the mean and variance of P, respectively. Observe that the moments of P formed from an estimated covariance matrix (sample covariance matrix) with finite sample support deviate significantly from the corresponding moments for the case of a known covariance matrix given by (2.1) and (2.2). For example with $K = 2M$, there is a 100% deviation of the mean of (3.6) from that of (2.1). Therefore, comparing an empirically formed GIP with the theoretical mean of (2.1) provides misleading results in that a finite data effect is ascribed to training data non-homogeneity.

We then study the representation of (3.2) in the limit of large K. For this purpose, we consider the characteristic function of R_2/K given by

$$\phi_{R_2/K}(j\omega) = E\left[\exp\left(-j\omega\frac{R_2}{K}\right)\right] = \frac{1}{\left(1 + \frac{j\omega}{K}\right)^{K-M+1}}. \tag{3.8}$$

For $K \to \infty$, we have $\lim_{K\to\infty} \phi_{R_2/K}(j\omega) = \exp(-j\omega)$. Taking the inverse Fourier transform, we have

$$\lim_{K\to\infty} f_{R_2/K}(r) = \delta(r-1). \tag{3.9}$$

Hence, for $K \to \infty$, R_2/K becomes unity with probability one. Thus, the GIP for this case is simply R_1 and hence, follows a chi-squared distribution with M complex degrees of freedom. Consequently, for $K \to \infty$, $E(P) = \sigma_P^2 = M$ corresponding to the known covariance matrix results. Hence, the GIP statistical representation given by (3.2) provides additional insights on the NHD. The numerator random variable corresponds to the GIP statistics for known covariance matrix. The denominator random variable succinctly embeds the deleterious effects of estimating the covariance matrix with finite sample support. Deviation of the normalized GIP statistics from the PDF of (3.5) can then be attributed to non-homogeneity of the training data.

Figure 1 shows the PDF of P' for several values of K with $M = 8$ for Gaussian interference statistics. Observe that the variance of P' decreases with increasing K. This is anticipated since $\widehat{\mathbf{R}} \to \mathbf{R}$ with probability 1 as $K \to \infty$. Therefore, the statistics of P' incur a dependence on K resulting from the use of finite sample support in estimating the covariance matrix.

The results presented in Fig. 2 correspond to the case of homogeneous training data. They show a comparison of the histogram of P' obtained from Monte-Carlo realizations using simulated data with the theoretically predicted PDF of P' obtained from (3.5). The results reveal good agreement between the theoretical prediction and the empirically generated values. The mean value of P, 15.957, obtained via 50,000 Monte-Carlo realizations compares well with the theoretically predicted value of 16.

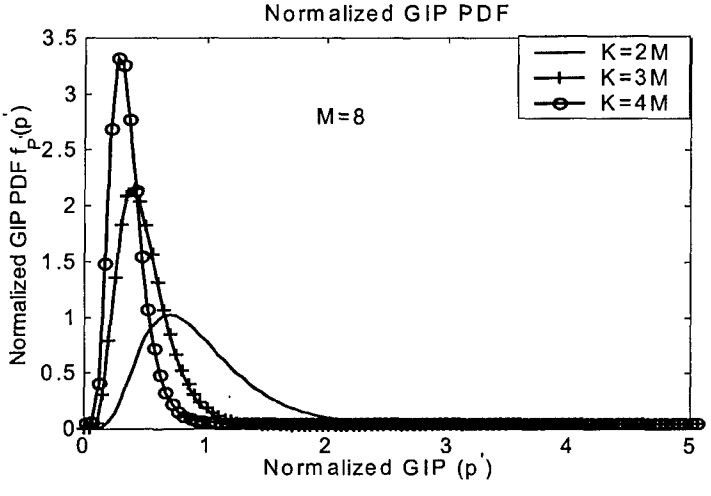

Fig. 1. Normalized GIP PDF.

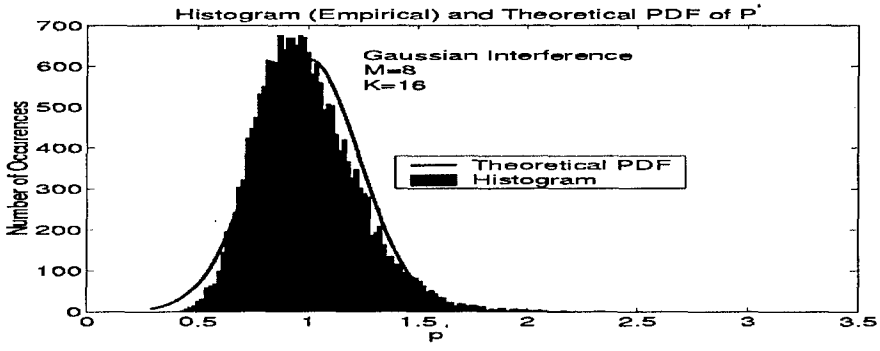

Fig. 2. Empirical and theoretical GIP PDF.

4. Non-homogeneity detector

We now present two methods for selecting homogeneous data from a set of training data. The first method exploits the central-F distribution of P' given by (3.5) to construct a formal goodness-of-fit test, while the second method relies upon a comparison of empirically formed P' with the theoretical mean predicted by (3.6) and discarding those realizations for which P' deviates significantly from the theoretical mean. More precisely, the difference between the empirical realizations of P' and the theoretically calculated mean value is obtained for each realization of P'. This difference is then rank ordered and the training data realizations corresponding to the least deviation from the theoretical mean are retained for subsequent use in STAP algorithms. The cumulative distribution function of P' is given by

$$\Pr(P' \leqslant r) = 1 - \text{betainc}\left(\frac{1}{r+1}, M, L\right), \tag{4.1a}$$

where

$$\text{betainc}(x, m, n) = \frac{1}{\beta(m,n)} \int_0^x w^{m-1}(1-w)^{n-1}\, dw. \tag{4.1b}$$

The goodness-of fit test consists of determining whether realizations of P' formed from a given set of training data are statistically consistent with the PDF of (2.1). For this purpose a suitable type-I error, α, is chosen. More precisely, α is simply the probability of incorrectly rejecting the hypothesis that a given realization of P' is statistically consistent with the PDF of (3.5). Specifically, we seek a threshold, λ, such that

$$\alpha = \Pr(P' > \lambda) = 1 - \Pr(P' \leqslant \lambda) = \text{betainc}\left(\frac{1}{\lambda+1}, M, L\right), \tag{4.2}$$

where λ is determined from a numerical inversion of (4.2). The goodness-of-fit test consists of forming realizations of P' from a set of training data and rejecting those training data vectors for which P' exceeds λ. The second method is based on comparing the realizations of P with the theoretically predicted mean of P given by (3.6) and retaining those

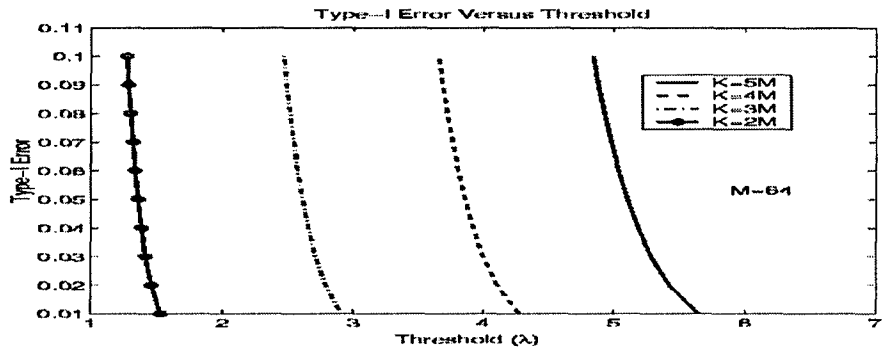

Fig. 3. Type-I error versus threshold.

realizations exhibiting the least deviation from the theoretically predicted mean of (3.6). Examples that illustrate the two approaches are presented. For a given training data set, a moving window approach is used to form realizations of P'. This approach is sub-optimal because it does not guarantee statistical independence of the realizations of P'. However, we adopt this approach due to the limited training data support. For the examples presented here, data from the MCARM program [13] corresponding to 16 pulses and 8 channels from acquisition '220' on Flight 5, cycle 'e' is used.

Figure 3 plots the type-I error (α) versus threshold for $M = 64$. Here different values of K are chosen to illustrate the threshold behavior. For each value of α, λ is determined from a numerical inversion of (4.2). For a given α, we observe an increase in λ for a given K.

The plot in Fig. 4 shows P' and λ corresponding to $\alpha = 0.1$ as a function of range. A moving window approach is used to obtain P' for each range cell considered. Non-homogeneity of the training data is seen in those range cells for which P' exceeds λ. Figure 5 plots the normalized GIP as a function of range. The normalized GIP theoretical mean is obtained from (3.6) with a simple normalization is also shown. Values of the normalized GIP, which exceed the theoretical mean correspond to non-homogeneous training data realizations.

5. Performance analysis of the AMF test

In this section, we consider the performance analysis of the AMF test [5,9,22] in non-homogeneous training data. The AMF test is given by

$$\Lambda = \frac{|\mathbf{s}^H \widehat{\mathbf{R}}^{-1}\mathbf{x}|^2}{|\mathbf{s}^H \widehat{\mathbf{R}}^{-1}\mathbf{s}|} \gtrless \lambda_{\mathrm{AMF}}, \tag{5.1}$$

where $\mathbf{s}$ is the spatio-temporal steering vector, $\mathbf{x}$ is the received data vector, $\widehat{\mathbf{R}}$ is the sample covariance matrix given by $\widehat{\mathbf{R}} = \frac{1}{K}\sum_i^K \mathbf{z}_i \mathbf{z}_i^H$ with $\mathbf{z}_i$ denoting independent identically distributed training data and λ_{AMF} is a threshold selected to obtain a desired probability of false alarm.

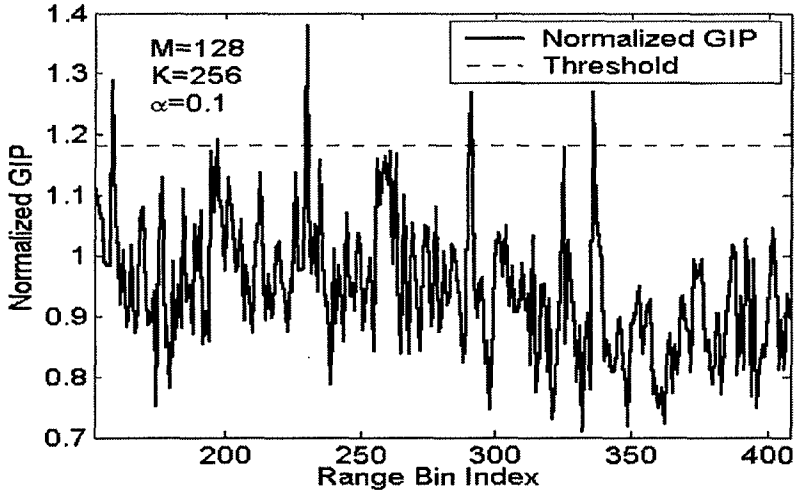

Fig. 4. Normalized GIP versus range.

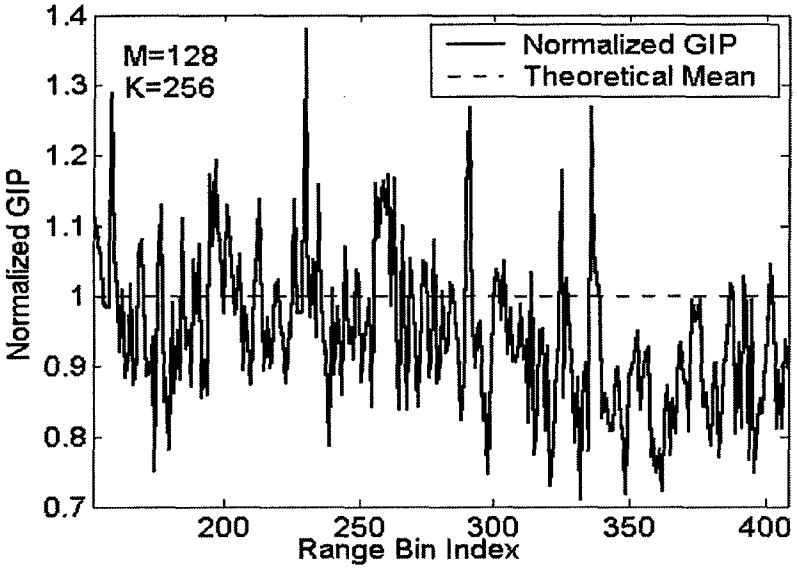

Fig. 5. Normalized GIP versus range.

For the case of homogeneous training data, analytical expressions for the probability of false alarm and probability of detection are given by [22]

$$P_{\text{fa}} = \int_0^1 \frac{f_\rho(\rho)\,d\rho}{(1+\rho\lambda_{\text{AMF}})^L}, \tag{5.2}$$

$$P_{\text{d}} = 1 - \int_0^1 \sum_{k=1}^{L} \binom{L}{k} \rho^k \lambda_{\text{AMF}}^k G_k\left[\frac{\rho b}{(1+\rho\lambda_{\text{AMF}})}\right] \frac{f_\rho(\rho)\,d\rho}{(1+\rho\lambda_{\text{AMF}})^L}, \tag{5.3}$$

where

$$f_\rho(\rho) = \frac{(1-\rho)^{M-2}\rho^L}{\beta(M-1, L+1)}, \qquad L = K - M + 1, \tag{5.4}$$

$$G_k(x) = \exp(-x) \sum_{n=0}^{k-1} \frac{x^n}{n!} \tag{5.5}$$

and 'b' is related to the output signal-to-noise ratio (SNR). For $K \to \infty$, the sample covariance matrix tends to the true clutter covariance matrix, $\mathbf{R}$. Consequently, the AMF test converges to the matched filter (optimal receiver in Gaussian disturbance) for large K. The expressions for the matched filter P_{fa} and P_{d} are given by [22]

$$P_{\text{fa}} = \exp(-\lambda_{\text{MF}}), \tag{5.6}$$

$$P_{\text{d}} = \exp(-A) \sum_{k=0}^{\infty} \frac{A^k}{k!} \left[1 - G_k(\lambda_{\text{MF}})\right], \tag{5.7}$$

where A is related to the output SNR and λ_{MF} is the matched filter threshold.

Figure 6 presents P_{d} versus output signal-to-interference plus noise ratio (SINR). Relevant test parameters are reported in the plot. The matched filter (MF) curve obtained from (5.7) corresponds to the optimal performance in Gaussian clutter. The P_{d} curve for the AMF operating in homogeneous Gaussian clutter follows from (5.3) and exhibits performance to within 3 dB of the MF. The AMF performance operating in non-homogeneous training data with and without NHD pre-processing is carried out by Monte-Carlo simulation. For this example, the training data contained thirty high-amplitude, mainbeam discrete targets located at various range cells and Doppler frequencies. Initial sample support for NHD pre-processing is $6M$. A sliding window approach is used to select a subset consisting of $4M$ training data realizations. Each GIP value obtained at a specific range cell is computed using $\widehat{\mathbf{R}}$ formed from $2M$ adjacent training data vectors. Previously, we noted the sub-optimality of this scheme. In practice, its use is dictated by training data size limitations. In this manner $4M$ GIP values are obtained. The NHD pre-processing used in this example is based on a comparison of the empirical GIP with its theoretical mean value given by (3.6). The training data used in forming $\widehat{\mathbf{R}}$ after NHD processing is obtained by sorting the GIP values and retaining $K = 2M$ realizations corresponding to the smallest GIP deviation from the theoretical mean of (3.6). Observe that the AMF performance in non-homogeneous clutter degrades severely. Also note that, for this case, NHD pre-processing restores the AMF performance to its analytical value.

Figure 7 shows a plot of the GIP versus range prior to NHD pre-processing for the simulated data used in carrying out the performance analysis of Fig. 6. Figure 8 shows a

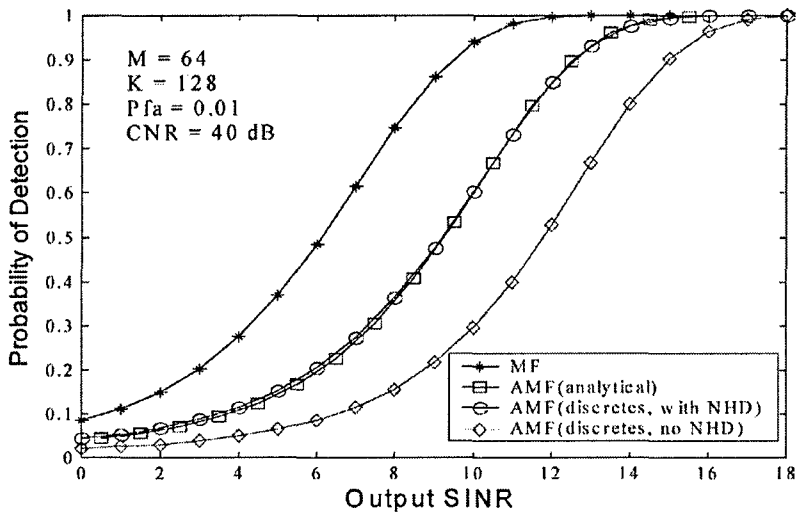

Fig. 6. Performance of the AMF 'with' and 'without' NHD.

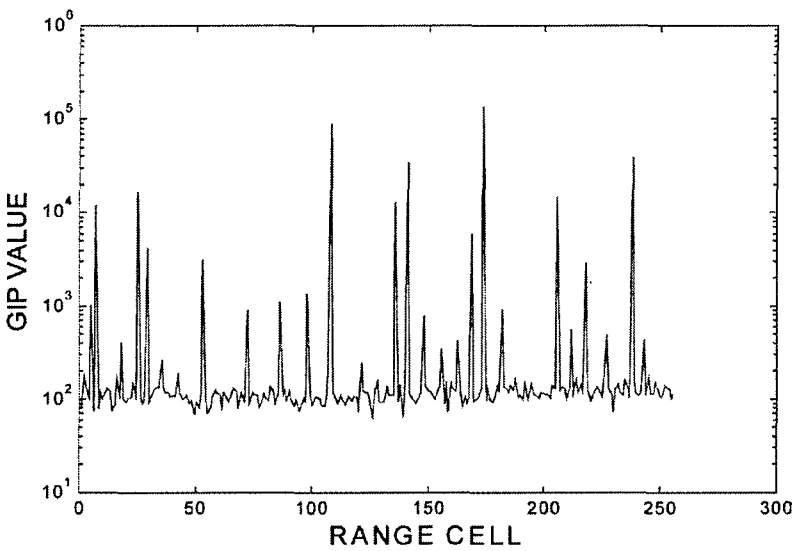

Fig. 7. GIP versus range.

plot of the sorted absolute value of the difference between the GIP and its theoretical mean versus range after NHD pre-processing for the example in Fig. 6. Observe the absence of discretes in the first $K = 2M$ range cells.

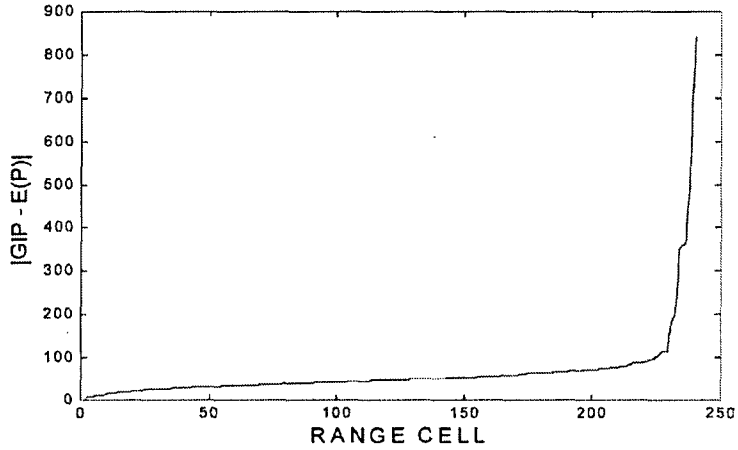

Fig. 8. Absolute value of difference between GIP and theoretical GIP mean vs range.

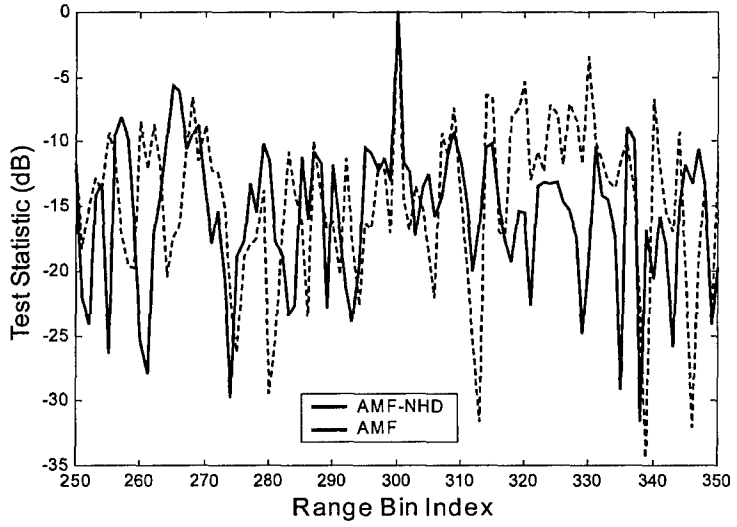

Fig. 9. Test statistic vs range.

Figure 9 depicts performance using measured data from the MCARM program [13]. For this case, it is not possible to present performance in terms of detection probability versus SINR. This is due to the fact that only one realization of target present data is available. Hence, we present a plot of the detection test statistic versus range. Since the AMF test statistic is an ad-hoc estimate of the output SINR, and since the probability of detection is a monotonically increasing function of the output SINR, this is an acceptable performance metric.

Table 1
AMF performance with measured data

Algorithm	ψ_1 (dB)	ψ_2 (dB)
AMF with NHD	13.25	5.68
AMF	11.83	3.38

Performance of the AMF without NHD processing degrades significantly in non-homogeneous clutter. Performance improvement is noted when the AMF is employed in non-homogeneous data with NHD pre-processing. Consequently, the use of NHD affords moderate performance improvement of the AMF test in non-homogeneous clutter. The performance with measured data is characterized by the ratio of the test statistic at the test cell to the mean of the test statistics formed from adjacent cells, ψ_1, and the ratio of the test statistic at the test cell to the highest test statistic formed from adjacent cells, ψ_2, respectively. Table 1 shows these values for the AMF test with and without NHD pre-processing.

6. Conclusions

This paper has made several significant contributions. First, we provided a statistical characterization of the GIP based NHD developed in [6,7,10,14,15]. We showed that the underlying GIP statistics deviate significantly when the unknown covariance matrix is estimated using finite sample support. A canonical representation for the GIP in terms of two statistically independent chi-square distributed random variables and the resulting central-F distribution for the normalized GIP were then used to construct goodness-of-fit tests, whose performance is presented using both simulated and measured data. Application of this method as a pre-processing method for training data selection in the adaptive matched filter algorithm (AMF) was presented. Performance of the AMF in contaminated training data degrades significantly. The use of our pre-processing method for training data selection restores the AMF performance to within 3 dB of the optimal matched filter (MF) performance. This fact is illustrated with simulated as well as measured data from the MCARM program. Future work will undertake extensive performance comparisons between covariance based STAP methods such as the AMF and the normalized adaptive matched filter (NAMF) [11] (with NHD pre-processing) and model-based parametric STAP tests such as the parametric adaptive matched filter (PAMF) [23], normalized parametric adaptive matched filter (N-PAMF) [18] and fast adaptive processors [25] in non-homogeneous interference backgrounds.

Acknowledgments

This work was supported by the Air Force Office of Scientific Research (AFOSR) under Project 2304E8 and by in-house research efforts at the U.S. Air Force Research Laboratory. Portions of this paper were presented at the 34th Asilomar Conference on Signals, Systems, and Computers, Pacific Grove, CA, November 2000 and at the National Radar Conference (RADAR-2001), Atlanta, GA, May 2001.

Appendix A. Stochastic representation for the normalized GIP

Let $\mathbf{Z}$ denote a data matrix whose columns are the previously defined $\mathbf{z}_i$, $i = 1, 2, \ldots, K$. The maximum likelihood estimate of the covariance matrix is given by $\widehat{\mathbf{R}} = \frac{1}{K}\mathbf{Z}\mathbf{Z}^H$. The data matrix $\mathbf{Z}$ and the test data vector $\mathbf{x}$ admit a representation of the form

$$\begin{aligned} \mathbf{Z} &= \mathbf{R}^{1/2}\mathbf{Y}, \\ \mathbf{x} &= \mathbf{R}^{1/2}\mathbf{y}, \end{aligned} \tag{A.1}$$

where $\mathbf{Y}$ is a data matrix whose columns $\mathbf{y}_i$, $i = 1, 2, \ldots, K$, are iid $CN(\mathbf{0}, \mathbf{I})$ random vectors and $\mathbf{y}$ is a $CN(\mathbf{0}, \mathbf{I})$ random vector which is statistically independent of $\mathbf{Y}$. Hence, the normalized GIP is expressed as

$$P' = \mathbf{y}^H \mathbf{S}_y^{-1} \mathbf{y}, \tag{A.2}$$

where $\mathbf{S}_y = \frac{1}{K}\mathbf{Y}\mathbf{Y}^H$. Next, we use a Householder transformation defined by $\mathbf{A} = (\mathbf{I} - 2\mathbf{u}\mathbf{u}^H/\mathbf{u}^H\mathbf{u})$, where $\mathbf{u} = \mathbf{y} - \|\mathbf{y}\|\mathbf{e}$ and $\mathbf{e} = [1\,0\,0\ldots0]^T$ so that $\tilde{\mathbf{y}} = \mathbf{A}\mathbf{y}$. Also let $\widetilde{\mathbf{Y}} = \mathbf{A}\mathbf{Y}$. Since $\mathbf{A}\mathbf{A}^H = \mathbf{A}^H\mathbf{A} = \mathbf{I}$, it follows that the statistics of $\widetilde{\mathbf{Y}}$ are identical to that of $\mathbf{Y}$. Consequently, the normalized GIP is expressed as

$$P' = \tilde{\mathbf{y}}^H \mathbf{S}_{\tilde{y}}^{-1} \tilde{\mathbf{y}}. \tag{A.3}$$

Furthermore, we partition

$$\widetilde{\mathbf{Y}} = \begin{bmatrix} \mathbf{y}_1^H \\ \mathbf{Y}_{11}^H \end{bmatrix},$$

where $\mathbf{y}_1^H$ is the first row of $\widetilde{\mathbf{Y}}$ and $\mathbf{Y}_{11}^H$ denotes the $(M-1) \times K$ matrix formed from the remaining rows of $\widetilde{\mathbf{Y}}$. Consequently,

$$\mathbf{S}_{\tilde{y}} = \begin{bmatrix} \mathbf{y}_1^H\mathbf{y}_1 & \mathbf{y}_1^H\mathbf{Y}_{11} \\ \mathbf{Y}_{11}^H\mathbf{y}_1 & \mathbf{Y}_{11}^H\mathbf{Y}_{11} \end{bmatrix}. \tag{A.4}$$

Also, $\mathbf{S}_{\tilde{y}}^{-1}$ admits a representation of the form

$$\mathbf{S}_{\tilde{y}}^{-1} = \begin{bmatrix} \mathbf{S}_{11} & \mathbf{S}_{12} \\ \mathbf{S}_{21} & \mathbf{S}_{22} \end{bmatrix}. \tag{A.5}$$

Finally, the normalized GIP is expressed as

$$P' = \|\mathbf{y}\|^2 \mathbf{S}_{11}.$$

However, from the matrix inversion lemma it follows that $\mathbf{S}_{11} = (\mathbf{y}_1^H\mathbf{P}_\perp\mathbf{y}_1)^{-1}$, where $\mathbf{P}_\perp = \mathbf{I} - \mathbf{Y}_{11}(\mathbf{Y}_{11}^H\mathbf{Y}_{11})^{-1}\mathbf{Y}_{11}^H$. Since $\mathbf{Y}_{11}(\mathbf{Y}_{11}^H\mathbf{Y}_{11})^{-1}\mathbf{Y}_{11}^H$ is a projection matrix of rank $M-1$, it follows that $\mathbf{P}_\perp$ is a projection matrix of rank $K - M + 1$. Consequently,

$$\mathbf{y}_1^H\mathbf{P}_\perp\mathbf{y}_1 = \sum_{i=1}^{K-M+1} |y(i)|^2, \tag{A.6}$$

where $y(i) \sim CN(0, 1)$. Hence, $\mathbf{S}_{11}$ is simply the reciprocal of a chi-squared distributed random variable with $(K - M + 1)$ complex degrees-of-freedom. Also, since $\mathbf{y}$ is a $CN(\mathbf{0}, \mathbf{I})$ random vector, $\|\mathbf{y}\|^2$ is a chi-squared distributed random variable with M complex degrees of freedom. Consequently, the representation of (3.2) follows.

References

[1] Y.I. Abramovich, Analysis of a direct adaptive tuning method for interference compensation systems with auxiliary linear constraints, Soviet J. Commun. Technol. Electron. 35 (1) (1990) 30–37 (English translation of Radioteknika i Elektronika).

[2] Y.I. Abramovich, Convergence analysis of linearly constrained {SMI} and {LSMI} adaptive algorithms, in: Proceedings of ASSPCC-2000, Lake Louise, Canada, 2000, pp. 255–259.

[3] Y.I. Abramovich, V.N. Mikhaylyukov, I.P. Malyavin, Test of interference stationarity in adaptive filtering systems, Soviet J. Commun. Technol. Electron. 37 (3) (1992) 1–10 (English translation of Radioteknika i Elektronika).

[4] T.W. Anderson, An Introduction to Multivariate Statistical Analysis, Wiley, New York, 1958.

[5] L. Cai, H. Wang, On adaptive filtering with the CFAR feature and its performance sensitivity to non-Gaussian interference, in: Proceedings of the 24th Annual Conference on Information Sciences and Systems, Princeton, NJ, 1990, pp. 558–563.

[6] P. Chen, On testing the equality of covariance matrices under singularity, Technical Report, AFOSR Summer Faculty Research Program, Rome Laboratory, August 1994.

[7] P. Chen, Partitioning procedure in radar signal processing problems, Technical Report, AFOSR Summer Faculty Research Program, Rome Laboratory, August 1995.

[8] P. Chen, W. Melvin, M. Wicks, Screening among multivariate normal data, J. Multivariate Anal. 69 (1999) 10–29.

[9] W.S. Chen, I.S. Reed, A new CFAR detection test for radar, Digital Signal Process. (1991) 198–214.

[10] B. Himed, Y. Salama, J.H. Michels, Improved detection of close proximity targets using two-step NHD, in: Proceedings of the International Radar Conference, Alexandria, VA, 2000.

[11] S. Kraut, L.L. Scharf, L.T. McWhorter, Adaptive subspace detectors, IEEE Trans. Signal Process. SP-49 (2001) 1–16.

[12] S. Kraut, L.L. Scharf, L.T. McWhorter, Adaptive subspace detectors, IEEE Trans. Signal Process. 49 (1) (2001) 1–16.

[13] MCARMDATA, http://128.132.2.229, Data from the Multi-Channel Airborne Radar Measurement Program of the U.S. Air Force Research Laboratory, Rome, NY.

[14] W. Melvin, M. Wicks, Improving practical space-time adaptive radar, in: Proceedings of the IEEE National Radar Conference, Syracuse, NY, 1997.

[15] W. Melvin, M. Wicks, R. Brown, Assessment of multichannel airborne radar measurements for analysis and design of space–time adaptive processing architectures and algorithms, in: Proceedings of the IEEE National Radar Conference, Ann Arbor, MI, 1996.

[16] W.L. Melvin, Space-time adaptive radar performance in heterogeneous clutter, IEEE Trans. Aerospace Electron. Systems 36 (2) (2000) 621–633.

[17] W.L. Melvin, J.R. Guerci, M.J. Callahan, M.C. Wicks, Design of adaptive detection algorithms for surveillance radar, in: Proceedings of the International Radar Conference, Alexandria, VA, 2000.

[18] J.H. Michels, B. Himed, M. Rangaswamy, Performance of STAP tests in Gaussian and compound-Gaussian clutter, Digital Signal Process. 10 (4) (2000) 309–324.

[19] R. Nitzberg, An effect of range-heterogeneous clutter on adaptive Doppler filters, IEEE Trans. Aerospace Electron. Systems 26 (3) (1990) 475–480.

[20] M. Rangaswamy, B. Himed, J. Michels, Statistical analysis of the nonhomogeneity detector, in: Proceedings of the 34th Asilomar Conference on Signals, Systems, and Computers, Pacific Grove, CA, 2000.

[21] M. Rangaswamy, D. Weiner, A. Ozturk, Non-Gaussian random vector identification using spherically invariant random processes, IEEE Trans. Aerospace Electron. Systems AES-29 (1993) 111–124.

[22] F. Robey, D. Fuhrmann, E. Kelly, R. Nitzberg, A CFAR adaptive matched filter detector, IEEE Trans. Aerospace Electron. Systems AES-28 (1992) 208–216.

[23] J.R. Roman, M. Rangaswamy, D. Davis, Q. Zhang, B. Himed, J.H. Michels, Parametric adaptive matched filter for airborne radar applications, IEEE Trans. Aerospace Electron. Systems AES-36 (2000) 677–692.

[24] M. Siotani, T. Hayakawa, Y. Fujikoshi, Modern Multivariate Statistical Analysis, American Science, Ohio, 1985.

[25] M. Steiner, K. Gerlach, Fast converging adaptive processor for a structured covariance matrix, IEEE Trans. Aerospace Electron. Systems AES-36 (2000) 1115–1126.

Muralidhar Rangaswamy received the PhD in electrical engineering from Syracuse University, Syracuse, NY, in 1992. He is currently employed as a senior electronics engineer at the Air Force Research Laboratory (AFRL), Hanscom AFB, MA, where he is conducting research in the area of phenomenology-based adaptive radar signal processing. Prior to this, he held positions in industry and academia. Dr. Rangaswamy has authored more than 40 journal and conference papers in the areas of his research. He has delivered invited presentations at numerous government, industrial, and academic forums. Dr. Rangaswamy is a co-inventor on two US patents and is a co-author of two book chapters. He is a Senior Member of the IEEE and regularly performs peer review of manuscripts submitted to several IEEE Transactions. Dr. Rangaswamy is actively involved in the sensor array and multichannel processing technical committee of the IEEE Signal Processing Society and has played a leading role in organizing numerous conferences, workshops, and short courses in the areas of his research. He received the postdoctoral research associate award from the National Research Council, USA, in 1993. At AFRL, he has received 12 scientific achievement awards.

James H. Michels has been conducting research and development analyses at the Air Force Research Laboratory (AFRL) in adaptive signal processing for radar applications. Over the past decade, he has pioneered the development of multichannel parametric model-based methods for space–time adaptive processing, change detection, and biomedical applications. He has over 50 papers in this technical area, five patents, and several patent applications pending. Dr. Michels received the PhD in electrical engineering in 1991 from Syracuse University, Syracuse, NY. In 1999, he was an IEEE Region I Award winner for "Contributions to Multi-channel Signal Processing." At AFRL, he has twice won the Charles Ryan Award for contributions to basic research and received the Chief Scientist Award for Best Published Paper in 1995. From August 1998 to August 1999, he was a visiting scientist at the former Defense Evaluation and Research Agency (DERA) in Malvern, England, sponsored by the Air Force Office of Scientific Research (AFOSR) Engineer and Scientist Exchange Program (ESEP).

Braham Himed received his BS degree from École Nationale Polytechnique of Algiers, Algeria, in 1984 and his MS and PhD from Syracuse University, Syracuse, NY, in 1987 and 1990, respectively, all in electrical engineering. From 1990 to 1991 he was an assistant professor in the Electrical Engineering Department at Syracuse University, where he taught graduate courses in analog and digital communications, digital signal processing, probability and random processes, Kalman filtering, and wireless communications. In 1991 he joined Adaptive Technology, Inc., Syracuse, NY, as a research engineer, where he was responsible for radar systems analyses and the analysis and design of antenna measurement systems. In 1994 he joined Research Associates for Defense Conversion, Marcy, NY, as a senior research engineer, where he was responsible for radar systems analyses, radar signal processing, detection and estimation of targets, clutter, and jamming mitigation. Currently, he is a senior research engineer with the US Air Force Research Laboratory, Sensors Directorate, Radar Signal Processing Branch, Rome, NY, where he is involved in bistatic airborne and space-borne phased array radar systems. His research interests include detection, estimation, multi-channel adaptive signal processing, time series analyses, array processing, space–time adaptive processing, hot clutter mitigation, and ground penetrating radar technology. Since 1993, he has also been an adjunct professor at Syracuse University. Dr. Himed is a senior member of the IEEE.